A New Simple-Structure Passive Lossless Snubber for DC_DC Boost Converters

Tayyebeh Shamsi, Majid Delshad, Ehsan Adib, and Mohammad Rouhollah Yazdani

***Abstract*—A new soft-switching boost converter with simple-structure passive lossless snubber is proposed in this paper. It shows various advantages as low cost, few auxiliary elements, and low voltage stress on the switch. The passive snubber circuit consists of an inductor, two capacitors, and two diodes. It provides zero current switching (ZCS) turn-on and zero voltage switching (ZVS) turn-off for the switch. The main diode turns on under ZVS and turns off under zero-voltage zero-current switching (ZVZCS), therefore reverse recovery problem is solved. Also, total efficiency and conducted electromagnetic interference (EMI) of the proposed converter compared to the conventional boost converters are improved. To prove it, a 220 W prototypes are implemented. The experimental results along with the theoretical analysis confirm an increase of 3% in efficiency of the proposed converter.**

***Index Terms*—passive lossless snubber, soft switching, zero current switching, zero voltage switching.**

I. INTRODUCTION

Pulse width modulated (PWM) converters have been widely used in various applications due to their fast transient response and high power density. Although, a high power density can be achieved by increasing the switching frequency, switching losses and electromagnetic interference (EMI) would be limiting factors. Therefore, the efficiency of the converter decreases as the frequency increases. To alleviate the hard switching issues, soft switching techniques have been proposed for dc-dc switching converters, where snubber circuits with active and passive type can be utilized.

The active snubber contains a switch together with passive elements [1-7]. In [1], the auxiliary circuit only consists of an active switch and a clamp capacitor to provide zero-current switching (ZCS) condition for the main switch. In [2], the main switch turns on and off under ZCS and zero-current transition (ZCT) condition. Although active snubber circuits work better than passive snubber circuits in switching loss point of view, they suffer from high cost of the auxiliary switch and the complexity of control and power circuits.

On the other hand, passive snubber circuit can achieve a soft switching by using passive components such as resistors, inductors, capacitors, and diodes. The RCD (resistor-capacitor-diode) circuit is the simplest type of a passive snubber circuit [8], [9] and reduces the voltage-stress across the switch during turn-off period. Despite these two advantages, power dissipation of resistors in RCD snubbbers limits low power applications and thus reduces the efficiency. So, the non-dissipative LCD (inductor-capacitor-diode) snubbers are introduced to achieve high efficiency, low switching loss and capablility for higher power conversion [10-23, 26].

In [10-14], [23] the number of components are relatively high in snubber circuit. The proposed snubber in [10] and [11] uses two seperate cores for implementing the inductors which affects the size of the converter. The proposed passive snubber in [13] uses a saturable inductor that leads to voltage ringing when the switch turns off. In [14], the switch and auxiliary diodes are suffering from voltage and current stress, respectively. In [15], a simple passive snubber is used to provide a soft switching condition. However, due to the presence of series coupled inductors with the switch, the voltage ringing results in the switch turn off. In [16], the current passes through the coupled snubber inductors freewheels through the converter switch resulting in high conduction losses. The coupled inductors in [15], [17], make undesired resonances.

On the other hand, there are lossless passive snubber circuits with few numbers of elements for dc-dc boost converters, but their main problem is that soft switching condition is not provided for the switches at turn-off instant [19], [20]. In some cases, the proposed passive snubber introduces extra voltage stress on the switch during the operating range [14-17]. For instance, in [22], the circulation loss has been increased since the stored energy in the capacitor of the snubber is delivered to the input voltage.

In this paper, a new lossless passive snubber is proposed for dc-dc boost converters without increasing the voltage stress. The proposed converter has a few number of components with no coupled inductors. The ZCS turn-on and ZVS turn-off of the switch has been achieved. All diodes including main and auxiliary ones turn on and off under a soft switching condition. The presented converter is comprehensively analyzed and meanwhile the operating modes are discussed in section II. Section III describes the design procedure. In section IV, the experimental results are presented. Conducted EMI of the boost converter with proposed snubber cell is evaluated in section V. Finally conclusions are given in Section VI.

Manuscript received Month xx, 2xxx; revised Month xx, xxxx; accepted Month x, xxxx. This work was supported in part by the … Department of xxx under Grant (sponsor and financial support acknowledgment goes here).

T. Shamsi, M. Delshad and M.R. Yazdani are with the Department of Electrical Engineering, Isfahan (Khorasgan) Branch, Islamic Azad University, Isfahan, Iran (email: tayyebeh.shamsi1@gmail.com, delshad@khuisf.ac.ir, mro.yazdani@gmail.com)

E. Adib are with the Department of Electrical and Computer Engineering, Isfahan University of Technology, Isfahan, Iran (e-mail: e.adib@cc.iut.ac.ir)

M. Delshad is with the Department of Electrical Engineering, Isfahan (Khorasgan) Branch, Islamic Azad University, Isfahan, Iran (corresponding author to provide phone: +98-313-5002700; fax: +98-313-5004060; e-mail: delshad@khisf.ac.ir).

II. CIRCUIT ANALYSIS

The schematic of the proposed boost converter is shown in Fig. 1.It includes a boost converter and an auxiliary circuit, consisting of a snubber inductance Ls, a snubber capacitor C_2, a buffer capacitor C_1, and two auxiliary diodes D_1 and D_2. The L_S provides ZCS condition at turn-on and C_2 with C_1 provide ZVS condition at turn-off instant of the switch. Also C_1, D_1 and D_2 recover the stored energy of the snubber to the output. The main operation waveform and equivalent circuit schemes of the proposed converter are given in Fig. 2 and Fig. 3 respectively. To analyze the circuit, the following assumptions are considered during on switching cycle:

a) The boost inductor L_{in} is large enough, thus the input current I_{in} is constant in the switching cycle.
b) The output capacitor C_o is large enough, thus the output voltage V_o is constant.

As is seen, different modes occur in the steady state of one switching cycle as below.

Mode 1 [t_0–t_1]: Before this mode, the switch is off and D_o is conducting input current and $V_{C2}=V_o$, $V_{C1}=0$. At $t=t_0$ the switch turns on with zero current condition because L_s limits the rate of rising of the switch current. The current of the inductor L_S increases linearly whereas the current of diode D_o decreases. V_o is placed across L_s so the current of the L_s and D_o are given by

$$i_{Ls} = i_s = \frac{V_o}{L_s}(t - t_0) \tag{1}$$

$$i_{Do} = I_{in} - \frac{V_o}{L_s}(t - t_0) \tag{2}$$

This mode ends when the switch current reaches I_{in}. Hence,

$$t - t_0 = \frac{L_s I_{in}}{V_o} \tag{3}$$

Mode 2 [t_1-t_2]: At t_1, the current of the main diode is equal to zero and because of C_2, D_o turns off under zero voltage zero current switching (ZVZCS). A resonance begins between L_s and C_2, so the current of L_s increases while the voltage of C_2 decreases in sinusoidal. The current of L_s is the total current of I_{C2} and I_{in}. Assuming the initial condition of $V_{C2}(t_1)=V_o$ and $i_{Ls}(t_1)=I_{in}$, the following equations are obtained.

$$i_{Ls} = V_o\sqrt{\frac{C_2}{L_s}}\sin(\omega_1(t - t_1)) + I_{in} \tag{4}$$

$$V_{c2} = V_o \cos(\omega_1(t - t_1)) \tag{5}$$

$$\omega_1 = \frac{1}{\sqrt{L_s C_2}} \tag{6}$$

This mode ends when $V_{C2}(t)$ equals zero. Thus, the duration of this mode is

$$\Delta t_2 = t_2 - t_1 = \pi\frac{\sqrt{L_s C_2}}{2} \tag{7}$$

Mode 3 [t_2-t_3]: At the beginning of this mode, as the voltage of C_2 equals zero, D_1 starts conducting at ZVS condition. The resonance between C_2 and L_s continues which discharges C_2 voltage. Also, a new resonance between C_1 and L_s occurs which increases C_1 voltage. At $t=t_2$, $i_s=i_{Ls}$, $V_{C2}(t_2)=0$ and $V_{C1}(t_2)=0$. The following equations are established.

$$V_{C1} = -V_{C2}\,,\quad i_{C1} = \frac{-C_1}{C_2} i_{C2} \tag{8}$$

$$I_{in} + i_{C1} - i_{C2} = i_{LS} \tag{9}$$

$$I_1 = i_{Ls}(t_2) = V_o\sqrt{\frac{C_2}{L_S}} + I_{in} \tag{10}$$

This mode ends when the switch turns off. Since the total voltage of C_1 and C_2 is equal to zero at this instant, the switch turns off at ZVS condition. The equations of this mode can be written by using the initial condition of (8) and (9).

$$V_{C1} = V_o\frac{\sqrt{C_1 C_2}}{C_1 + C_2}\sin(\omega_2(t - t_2)) \tag{11}$$

$$V_{C2} = -V_0\frac{\sqrt{C_1 C_2}}{C_1 + C_2}\sin(\omega_2(t - t_2)) \tag{12}$$

$$i_{Ls} = V_0\sqrt{\frac{C_2}{L_S}}\cos\big(\omega_2(t - t_2)\big) + I_{in} \tag{13}$$

$$\omega_2 = \frac{1}{\sqrt{L_S C_1}} \tag{14}$$

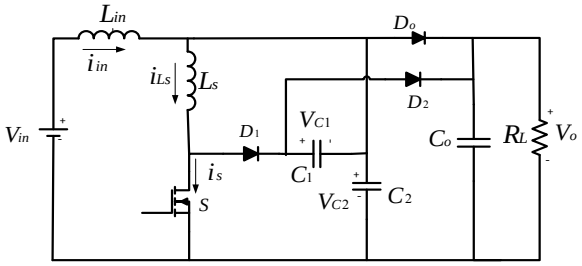

Fig. 1 Circuit scheme of the converter with the proposed passive snubber

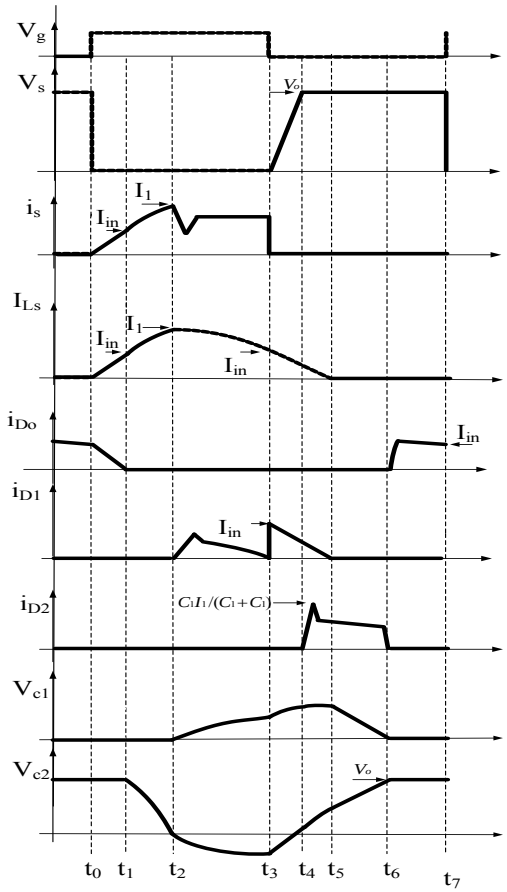

Fig. 2 Key waveforms of the proposed soft switching boost

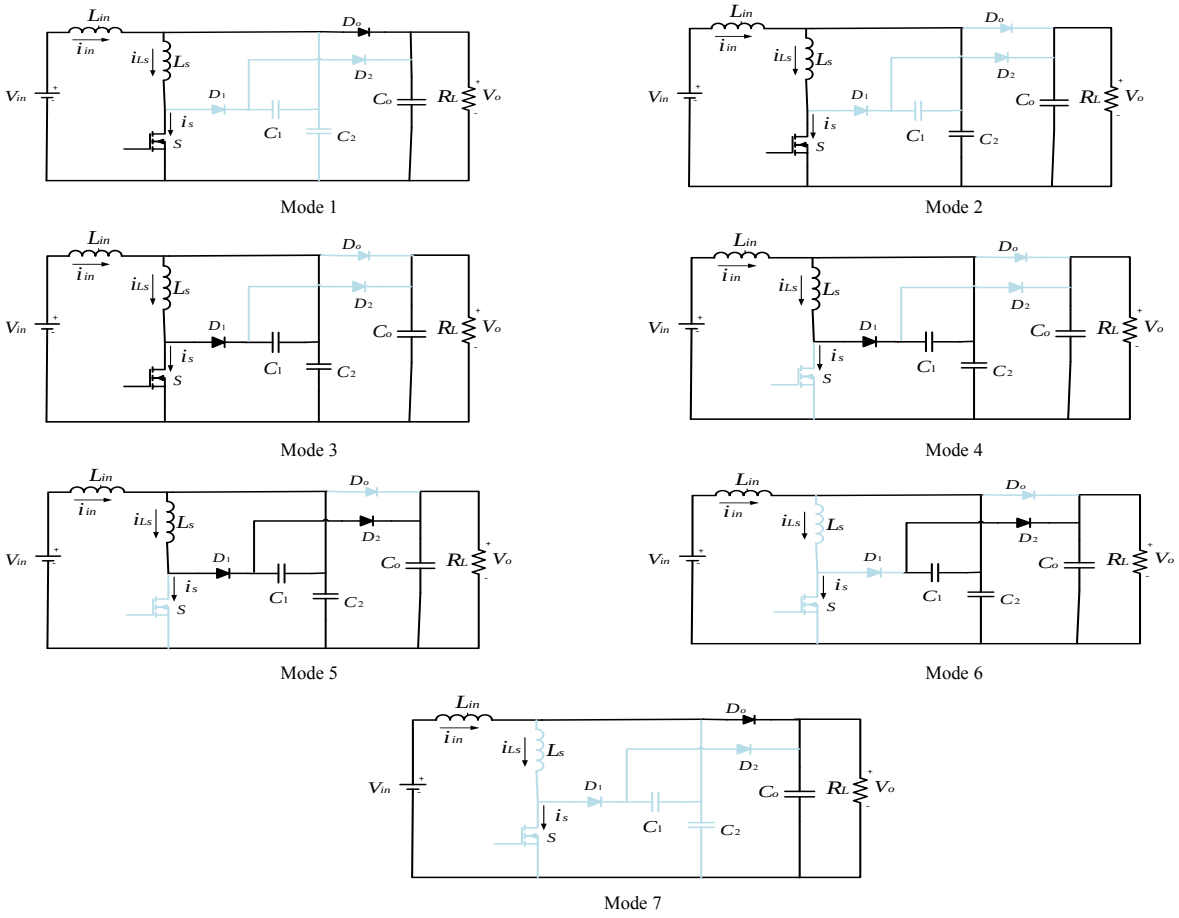

Fig. 3 Equivalent circuit schemes of the operation modes

At the end of this mode, when the switch turns off, i_{C1} and i_{C2} are zero and i_{Ls} =I_{in}. So, the duration of this mode can be obtained.

$$\Delta t_3 = (t_3 - t_2) = \frac{\pi\sqrt{L_S C_1}}{2} \tag{15}$$

The voltage of C_2 is negative in the mode 3 ($t_2<t<t_3$) and in t_3, it reaches its maximum value. The sum of this voltage with the output voltage is the maximum voltage of diode D_0.

Mode 4 [t_3-t_4]: After the switch turns off at t_3, the resonance between L_s and C_2 stops, I_{in} passes through C_2 and thus the voltage of capacitor C_2 increases in a linear manner. The resonance started between L_s and C_1 continues; so, the current of L_s decreases while the voltage of C_1 increases in a resonant manner while i_{Ls} is equal to i_{C1}. When the sum of the total voltage of C_1 and C_2 reaches to the voltage of V_o, D_2 turns on and this mode ends. For this mode the initial conditions at t=t_3 are

$$V_{C1}(t_3) = V_o \frac{\sqrt{C_1 C_2}}{C_1 + C_2} \tag{16}$$

$$V_{C2}(t_3) = -V_o \frac{\sqrt{C_1 C_2}}{C_1 + C_2} \tag{17}$$

$$i_{Ls}(t_3) = I_{in} \tag{18}$$

The values of V_{c1} and V_{c2} voltage and i_{Ls} current at this mode are as follow

$$V_{C1} = \frac{1}{C_1} I_{in}(t - t_3) + \frac{V_o\sqrt{C_1 C_2}}{C_1 + C_2} cos(\omega_2(t - t_3)) \tag{19}$$

$$V_{C2} = \frac{1}{C_2} I_{in}(t - t_3) - \frac{V_o\sqrt{C_1 C_2}}{C_1 + C_2} \tag{20}$$

$$i_{Ls} = i_{C1} = I_{in} - V_0 \frac{C_1\sqrt{\frac{C_2}{L_s}}}{C_1 + C_2} sin\big(\omega_2(t - t_3)\big) \tag{21}$$

At the end of this mode, at t_4 the following equation is established.

$$\frac{i_{C2}}{i_{C1}} = \frac{C_1}{C_2} \tag{22}$$

So, the duration of this mode can be calculated as:

$$\Delta t_4 = (t_4 - t_3) = \frac{1}{\omega_2} sin^{-1}\left(\frac{I_{in}(C_1 - C_2)}{C_1^2 V_o \frac{\sqrt{\frac{C_2}{L_s}}}{C_1 + C_2}}\right) \tag{23}$$

Mode 5 [t_4-t_5]: This mode starts when D_2 turns on under ZVS condition. The total voltage of C_1 and C_2 is clamped by D_2. In this mode, the inductor of L_s resonances with both capacitors C_1 and C_2. The voltages of both capacitors increase while the current of L_s decreases. This mode ends when the energy of L_s is transferred completely so, i_{Ls} becomes zero. At t=t_4, i_{Ls}=I_{in} (C_2/C_1). The equations of this mode are:

$$V_{C1} + V_{C2} = V_o \tag{24}$$

$$\frac{i_{C2}}{i_{C1}} = \frac{-C_1}{C_2} \tag{25}$$

$$V_{C1} = \frac{I_{in}}{C_1 + C_2}\left(\frac{C_2}{C_1}\right)\left[\frac{C_2}{C_1}\sqrt{L_s C_2}\, sin\big(\omega_1(t - t_4)\big) - (t - t_4)\right] \tag{26}$$

$$V_{C2} = V_o - \frac{I_{in}}{C_1 + C_2}\left(\frac{C_2}{C_1}\right)\left[\frac{C_2}{C_1}\sqrt{L_s C_2}\, sin(\omega_1(t - t_4) - (t - t_4)\right] \tag{27}$$

$$i_{Ls} = I_{in}\frac{C_2}{C_1}cos\big(\omega_1(t - t_4)\big) \tag{28}$$

The duration of this mode is:

$$\Delta t_5 = t_5 - t_4 = \frac{\pi\sqrt{L_s C_2}}{2} \tag{29}$$

Mode 6 [t_5-t_6]: At t_5 the current of L_s becomes zero, and D_1 turns off under ZCS in this mode, C_1 and C_2 are discharged and charged respectively with I_{in} in a linear manner. At the end of this mode, the voltages of C_1 and C_2 equal to zero and the voltage of output capacitor C_o respectively. For this mode $i_{lS}(t_5) = 0$, V_{C1} and V_{C2} can be calculated with the following equations.

$$V_{C1}(t_5) = -\frac{I_{in}}{C_1}(t - t_6) + \frac{I_{in}}{C_1 + C_2}\left(\frac{C_2}{C_1}\right)\sqrt{L_s C_2}\left(\frac{C_2}{C_1} - \frac{\pi}{2}\right) \tag{30}$$

$$V_{C2}(t_5) = \frac{I_{in}}{C_1}(t - t_6) + V_o - \left[\frac{I_{in}}{C_1 + C_2}\left(\frac{C_2}{C_1}\right)\sqrt{L_s C_2}\left(\frac{C_2}{C_1} - \frac{\pi}{2}\right)\right] \tag{31}$$

At the end of this mode $V_{C1=0}$ thus the duration of this mode is:

$$\Delta t_6 = \frac{C_2}{C_1 + C_2}\sqrt{L_s C_2}\left(\frac{C_2}{C_1} - \frac{\pi}{2}\right) \tag{32}$$

Mode 7 [t_6-t_7]: At t_6, D_o is turned on under ZVS and the voltage of C_2 is clamped by the output voltage, so D_2 turns off under ZVS. The operation of the converter in this mode is the same as that of a conventional boost converter when its switch is off

$$\Delta t_7 = t_7 - t_6 = (1 - D)T - \Delta t_4 - \Delta t_5 - \Delta t_6 \tag{33}$$

III. Design Procedure

The procedure of selecting the filter inductor L_{in} and capacitor C_o is the same as that of a conventional method.

TABLE I
Voltage and current stresses of the switch and diodes of the proposed boost converter

Item	Voltage stress	Current stress
S	V_o	I_l
D_o	$V_o(1 + \frac{\sqrt{C_1 C_2}}{C_1 + C_2})$	I_{in}
D_1	V_o	I_{in}
D_2	V_o	I_{in}

In this section, a procedure to design the proposed snubber circuit is presented. It is important to properly select C_1, C_2, and L_s.

- Snubber inductor L_s

The inductor L_1 provides ZCS condition for the switch S at the turn on instant and is designed like any turn-on snubber inductor [24]. L_S can be calculated as

$$\boldsymbol{L_s > \frac{V_{sw,on} t_r}{I_{sw,on}}} \tag{34}$$

Where, $I_{sw,on}$ is the amplitude of the input current after turn on and t_r is the rise time of the switch current and $V_{sw,on}$ is the switch voltage before turn on.

- Snubber capacitor C_2

The capacitor C_1 provides ZVS condition for the switch S at the turn off instant and is designed like any turn-off snubber capacitor [24]. It can be calculated as

$$C_2 > \frac{I_{sw,off} t_f}{2V_{sw,off}} \tag{35}$$

where $I_{sw,off}$ is the amplitude of the input current before turn-off instant and t_f is the fall time of the switch current and $V_{sw,off}$ is the switch voltage after turn-off.

The minimum value of L_s and C_2 to ensure considerable reduction in switching losses can be calculated as (34) and (35) [24]. However, higher value of these elements results in better reduction of switching losses.

- Buffer capacitor C_1

The buffer capacitor C_1 should be selected to ensure the recovery of the stored energy of the inductor L_S. It can be calculated as:

$$\boldsymbol{\frac{1}{2}V_{C1,max}^2 C_1 + \frac{1}{2}V_{C2,max}^2 C_2 < \frac{1}{2}L_{Ls,max}^2 L_s} \tag{36}$$

Also, the voltage stress of C_1 can be calculated by using (36). The value of C_1 is normally larger than the value of C_2**.** The voltage and current stresses of the semiconductor components of the proposed boost converter are shown in Table I.

IV. Experimental Result

A prototype of a 220W boost converter with the proposed passive snubber cell has been implemented. The switching frequency is 100 kHz. The input and output voltages of the proposed converter are 48 and 96 V, respectively. IRF640 is used for the converter switch and MUR820 are chosen for all diodes.

TABLE II
Design parameters of the proposed converter

Parameter	value
Input voltage (V_{in})	48V
Output voltage (V_o)	96V
Switching frequency (f_{sw})	100kHz
Power MOSFET (S)	IRF640
Power diodes	MUR820
Inductor L_{in}	200µH
Inductor L_s	25µH
Capacitor C_1	100nF
Capacitor C_2	47nF

The design parameters of the proposed converter are shown in Table II. Fig. 4 shows the switching waveforms of the switch, including the switch voltage and current which confirm that S is turned on under ZCS and turned off under ZVS condition. The Voltage and current of D_o is shown in Fig. 5. As shown in this figure, the diode is turned on at ZVS and is turned off at ZVZCS condition. The voltage and current of D_1 and D_2 are shown in Fig. 6 and 7, respectively. Fig. 8 shows the current of D_1 and D_2 under same time frame. The experimental results confirm the operation of the proposed converter. The comparison of some of the soft switching converters with the proposed converter is presented in Table III. It should be noted that these efficiency values have been obtained in simulation. The proposed converter has a few numbers of components in comparison to converters of [13-14], [16], [18], [23] and the switch voltage stress is less than converters of [14-16]. In table IV, the losses of the proposed boost converter in comparison with a hard switching boost converter is presented. In this table, t_{on} and t_{off} are the turn-on and turn-off times of the converter switch, respectively. Also, I_{rr} is its reverse recovery current and t_{rr} is the diode reverse recovery time. Furthermore, C_{out} is switch output capacitance, R_{ds} is the switch on state resistance, I_{ave} is average current of main and auxiliary diodes, V_F is forward voltage of diodes. R_{Lin} and R_{Ls} are resistance of L_{in} and L_s respectively, and B is the flux density. Since the converter is in continuous conduction mode, core loss of L_{in} is negligible. The efficiency diagrams of the proposed boost converter and a hard switching boost converter are shown in Fig. 9. As shown in Fig. 9. The proposed efficiency is 96.4%. In comparison to the hard switching boost converter, the efficiency is improved by 3%. The efficiency diagram of the proposed boost converter versus input voltage is shown in Fig. 10.

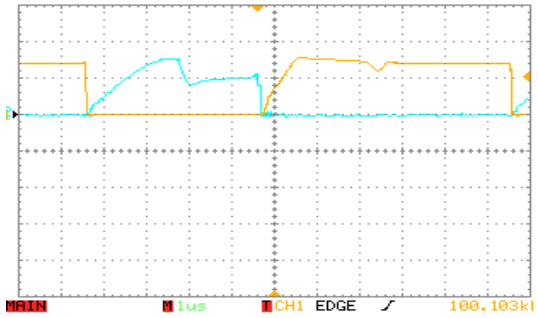

Fig. 4 (top) voltage and (bottom) current of the switch (voltage: 60 V/div; current: 5 A/div; time: 1 µs/div)

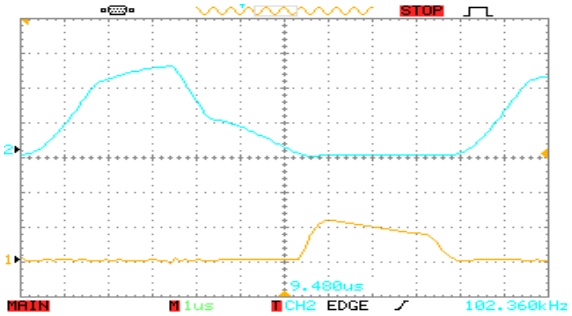

Fig. 5 (top) voltage and (bottom) current of the D_o (voltage: 50 V/div; current: 4.5 A/div; time: 1 µs/div)

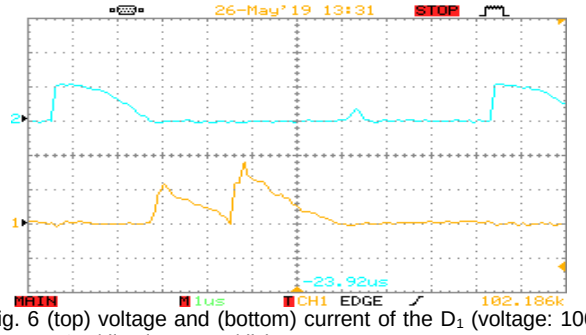

Fig. 6 (top) voltage and (bottom) current of the D_1 (voltage: 100 V/div; current: 3 A/div; time: 1 µs/div)

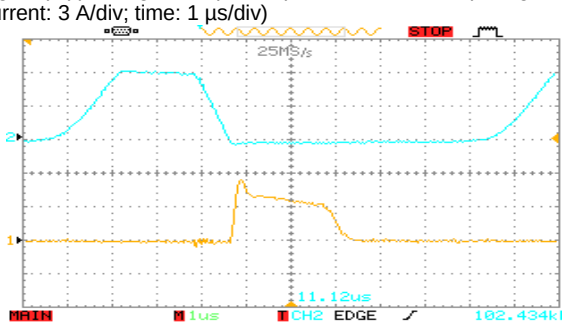

Fig. 7 (top) voltage and (bottom) current of the D_2 (voltage: 50 V/div; current: 3 A/div; time: 1 µs/div)

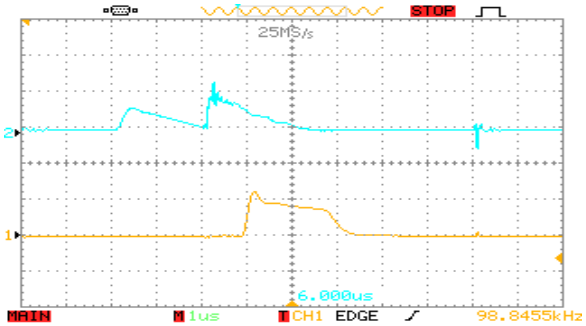

Fig. 8 currents of the (top) D_1 and (bottom) D_2 (current: 4.5 A/div; time: 1 µs/div

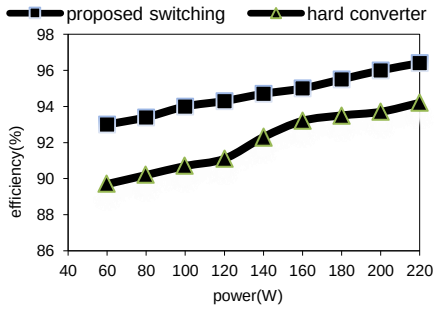

Fig. 9. Efficiency of the proposed boost converter compared with conventional hard-switching boost converter.

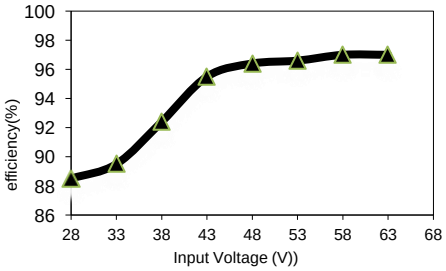

Fig. 10. Power efficiency as a function of input voltage.

TABLE III
Comparison between the proposed soft switching with some soft switching boost converters

converters	No. of auxiliary elements	Voltage stress of switch	Current stress of switch	Voltage stress of D_o	Current stress of D_o	Efficiency in simulation
[13]	9	V_O	$I_{in}+V_o\left(\sqrt{\frac{C_s}{L_s+L_{st}}}\sqrt{1-\frac{C_s}{C_{st}}}\right.$	----	----	----
[14]	8	$V_o(1+\sqrt{\frac{L_{s2}}{L_{s3}}})+I_o\sqrt{\frac{L_{s1}}{C_s}})$	$V_o\left(\sqrt{\frac{C_s}{L_s}}+I_o(1+\sqrt{\frac{L_{s1}}{L_{s2}}})\right.$	V_O	$i_{sw}=\frac{\bar{P}_o}{\eta V_{in}D}\left(1+\sqrt{\frac{L_{s1}}{L_{s2}}}\right)-\frac{\Delta I}{2}\left(1-\sqrt{\frac{L_{s1}}{L_{s2}}}\right)+V_o\sqrt{\frac{C_s}{L_{s2}}}$	96.7
[15]	4	$V_o(1+\frac{1}{n})$	$I_{in}+\frac{V_o}{\sqrt{\frac{L_{r1}}{C_r}}}$	V_O	$\sqrt{(\frac{n+1}{n})^2I_{in}^2+\frac{2(n+1)V_oI_{in}}{n^2\sqrt{\frac{L_{r1}}{c_r}}}}$	97.8
[16]	6	$V_o(1+\frac{1}{\sqrt{\frac{L_3}{L_2}}})$	$I_{in}+2V_o\left(\sqrt{\frac{C_1+C_2(\frac{L_2}{L_1})}{L_2+L_3}}\right.$	----	----	93.5
[18]	6	V_O	$I_1=\frac{P_o}{(1-D)V_o}+\frac{(1-D)D.T_{sw}}{L_{lk1}+L_{lk2}+[1-(\frac{n_2}{n_1})]^2.L_m}$	$V_o+(\frac{n_2}{n_1})V_{in}$	$I_1[1-(\frac{n_2}{n_1})]$	98.3
[21]	5	$\frac{V_o}{N+2}$	$I_{in}+\frac{2NI_o}{D}$	$\frac{(N+1)V_o}{N+2}$	$\frac{2NI_o}{D}$	96.2
[23]	8	$\frac{V_{in}}{1-d}$	$\frac{3I_o}{1-d}$	$\frac{V_{in}}{1-d}$	$\frac{I_o}{1-d}$	------
[26]	4	$V_o(1+\frac{1}{n})$	$1.5I_i$	V_o	$0.25\ I_i$	98.3
proposed	5	V_O	$I_{in}+V_o\sqrt{\frac{C_2}{L_s}}$	$V_o(1+\frac{\sqrt{C_1C_2}}{C_1+C_2})$	I_{in}	97.6

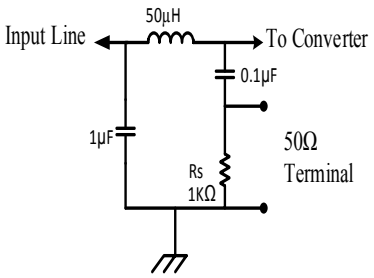

Fig. 11 a prototype circuit of CISPR22 LISN [25].

V. CONDUCTED EMI MEASUREMENT

In this section, the experimental measurements of the conducted EMI for the proposed converter are presented. The measurement setup includes a CICPR 22 line impedance stabilization network (LISN) and GWINSTEK GSP-830 spectrum analyser. The LISN and GWINSTEK GSP-830 spectrum analyser are inserted at the input of the converter [25] and on R_s respectively as shown in Fig. 11. The measured conducted EMI of the proposed converter is shown in Fig. 12.

According to CISPR 22 standard, the conducted EMI covers the frequency range of 150 kHz to 30 MHz. The main EMI peaks of the conventional boost converter and the proposed converter are about 84dBµV at 18MHz and 73dBµV at 16MHz, respectively. Therefore, the EMI peaks are reduced to 11dBµV. As shown in Fig. 12 the EMI is reduced in this frequency range by the use of the proposed lossless passive snubber. Also, the measured EMI shows that two main EMI peaks of the conventional boost converter are about 86.3dBµV and 84.3dBµV. The corresponding values for the proposed converter are 81.3dBµV and 74dBµV, which proves the boost converter with the proposed lossless passive snubber reduces the main EMI peaks about 5dBµV and 10dBµV. The EMI levels of the proposed converter and its hard switching counterpart for this frequency range are shown in Fig. 13. According to this figure, the EMI is decreased in many frequency ranges by using the proposed lossless passive snubber.

TABLE IV
Comparison of losses in hard switching boost converter and the proposed boost converter

Type of loss	Formula	Hard switching boost	Proposed converter
switching loss in S	$\frac{1}{2}V_o I_{in} f_{sw}(t_r + t_f + t_{rr})$	$\frac{1}{2}\times 96\times 5.4\times 10^5(145+110+195)\times 10^{-9}$	Zero
Parasitic capacitance loss in S	$\frac{1}{2}C_{out}V_o^2 f_{sw}$	$\frac{1}{2}\times 175\times 10^{-12}\times 96^2\times 10^5$	$\frac{1}{2}\times 175\times 10^{-12}\times 96^2\times 10^5$
conduction loss in S	$R_{ds}I^2_{RMS-s}$	$0.145\times(2.9)^2$	$0.145\times(4.4)^2$
conduction loss in diode D_o	$V_F I_{avg-Do}$	1×1.7	1×1.24
conduction losses in D_1	$V_F I_{avg-D1}$	N.A	1×1.15
conduction losses in D_2	$V_F I_{avg-D2}$	N.A	1×1.11
Conduction losses in L_{in}	$R_{Lin}I^2_{in}$	$23.68\times 10^{-3}\times(4.14)^2$	$23.68\times 10^{-3}\times(5.4)^2$
Conduction losses in L_{in}	$R_{Ls}I^2_{RMS-Ls}$	N.A	$3\times 10^{-3}\times(5.34)^2$
Core loss of L_s	$\frac{f_{sw}}{\left[\frac{1\times 10^9}{B^3}\right]+\left[\frac{1.1\times 10^8}{B^{2.3}}\right]+\left[\frac{1.9\times 10^6}{B^{1.65}}\right]}+1.9\times 10^{-13}B^2 f_{sw}^2$	0.0263	N.A
total loss		14.55W	7.16W

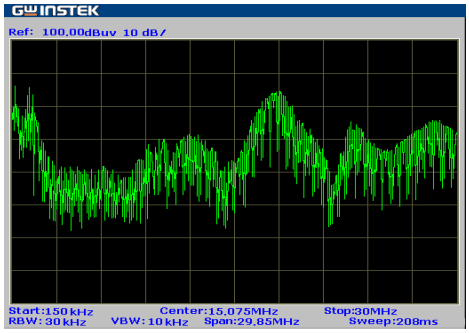

(a)

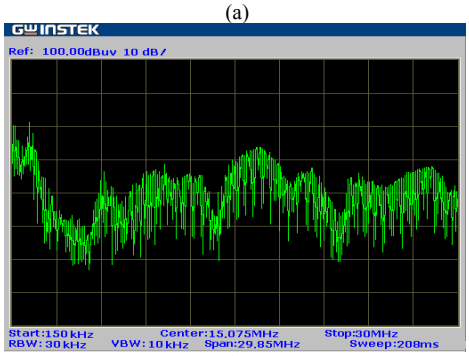

(b)

Fig. 12 (a) Measured conducted EMI of the conventional boost converter Vertical axis: 20-100dBμv; Horizontal axis: 15 kHz-30 MHz. (b) Measured conducted EMI of the boost converter with proposed snubber. Vertical axis: 20-100dBμv; Horizontal axis: 150 kHz-30 MHz.

VI. Conclusion

In this paper, a new simple passive lossless snubber for the boost converter with no voltage stress has been presented. This passive snubber uses a few components to provide ZCS turn-on and ZVS turn-off conditions for the power switch. Therefore, as the experimental results show, the efficiency of the converter has been improved. The soft switching condition is achieved for another element and thus the reverse recovery problems of the diodes are eliminated. The proposed converter is analysed and its operating modes are discussed. The experimental results are also presented which matches the theoretical results. Moreover, the conducted EMI of the proposed lossless passive snubber is measured and is compared to its hard switching counterpart, which shows the EMI levels are significantly reduced in many frequency ranges.

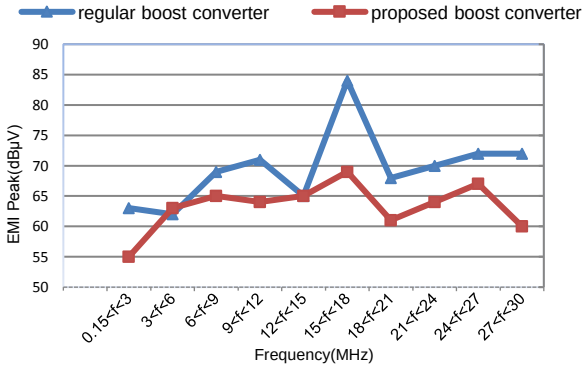

Fig. 13 EMI level of the proposed boost converter at different frequency ranges as compared to the hard-switching boost converter

References

[1] D. Murthy-Bellur and M. Kazimierczuk, "Zero-current-transition two-switch flyback pulse-width modulated DC-DC converter," *IET power electronics*, vol. 4, no. 3, pp. 288-295, Mar. 2011.

[2] S. Urgun, "Zero-voltage transition–zero-current transition pulsewidth modulation DC–DC buck converter with zero-voltage switching zero-current switching auxiliary circuit, " *IET power electronics*, vol. 5, no. 5, pp. 627-634, My. 2012.

[3] X. Zhang, L. Jiang, J. Deng, S. Li, and Z. Chen, "Analysis and design of a new soft-switching boost converter with a coupled inductor, " *IEEE Transactions on Power Electronics*, vol. 29, no. 8, pp. 4270-4277, Aug. 2014.

[4] L. Chen, H. Hu, Q. Zhang, A. Amirahmadi, and I. Batarseh, "A boundary-mode forward-flyback converter with an efficient active LC snubber circuit, " *IEEE Transactions on Power Electronics*, vol. 29, no. 6, pp. 2944-2958, Jun. 2014.

[5] B. Akın, "An improved ZVT–ZCT PWM DC–DC boost converter with increased efficiency," *IEEE Transactions on Power Electronics*, vol. 29, no. 4, pp. 1919-1926, Apr. 2014.

[6] N. Altintaş, A. F. Bakan, and I. Aksoy, "A novel zvt-zct-pwm boost converter," *IEEE Transactions on Power Electronics*, vol. 29, no. 1, pp. 256-265, Jan. 2014.

[7] N. S. Ting, I. Aksoy, and Y. Sahin, "ZVT-PWM DC–DC boost converter with active snubber cell," *IET power electronics*, vol. 10, no. 2, pp. 251-260, Feb. 2017.

[8] P. Meng, X. Wu, J. Yang, H. Chen and Z. Qian, "Analysis and design considerations for EMI and losses of RCD snubber in Flyback converter," *Applied Power Electronics Conference and Exposition (APEC)*, pp. 642-647, Feb. 2010.

[9] A. R. Vaz, F. L. Tofoli, "Practical design of a DC–DC buck converter using an RCD snubber", *Proc. Brazilian Power Electron. Conf.*, pp. 1-6, 2017.

[10] R. T. Li and H. S. h. Chung, "A passive lossless snubber cell with minimum stress and wide soft-switching range," *IEEE Transactions on Power Electronics*, vol. 25, no. 7, pp. 1725-1738, Jul. 2010

[11] K. Fujiwara and H. Nomura, "A novel lossless passive snubber for soft-switching boost-type converters," *IEEE Transactions on Power Electronics*, vol. 14, no. 6, pp. 1065-1069, Nov. 1999.

[12] E. S. da Silva, L. dos Reis Barbosa, J. B. Vieira, L. C. de Freitas, and V. Farias, "An improved boost PWM soft-single-switched converter with low voltage and current stresses," *IEEE Transactions on Industrial Electronics,* vol. 48, no. 6, pp. 1174-1179, Dec. 2001.

[13] R. T. Li, H. S. H. Chung, and A. K. Sung, "Passive lossless snubber for boost PFC with minimum voltage and current stress," *IEEE Transactions on Power Electronics*, vol. 25, no. 3, pp. 602-613, Mar. 2010.

[14] M. Mohammadi, E. Adib, and M. R. Yazdani, "Family of soft-switching single-switch PWM converters with lossless passive snubber," *IEEE Transactions on Industrial Electronics*, vol. 62, no. 6, pp. 3473-3481, Jun. 2015.

[15] M. R. Amini and H. Farzanehfard, "Novel family of PWM soft-single-switched DC–DC converters with coupled inductors," *IEEE Transactions on Industrial Electronics*, vol. 56, no. 6, pp. 2108-2114, Jun. 2009.

[16] T. Zhan, Y. Zhang, J. Nie, Y. Zhang, and Z. Zhao, "A novel soft-switching boost converter with magnetically coupled resonant snubber," *IEEE Transactions on Power Electronics,* vol. 29, no. 11, pp. 5680-5687, Nov. 2014.

[17] M. Khalilian, E. Adib, and H. Farzanehfard, "Family of single-switch soft-switching pulse-width modulation DC–DC converters with reduced switch stress," *IET Power Electronics*, vol. 7, no. 8, pp. 2182-2189, Apr. 2014.

[18] M. Esteki, M. Mohammadi, M. R. Yazdani, E. Adib, H. Farzanehfard, "Family of soft-switching pulse-width modulation converters using coupled passive snubber", *IET Power Electronics.*, vol. 10, no. 7, pp. 792-800, Jun. 2017.

[19] J.-J. Yun, H.-J. Choe, Y.-H. Hwang, Y.-K. Park, and B. Kang, "Improvement of power-conversion efficiency of a DC–DC boost converter using a passive snubber circuit," *IEEE Transactions on Industrial Electronics*, vol. 59, no. 4, pp. 1808-1814, Apr. 2012.

[20] J.-M. Kwon, W.-Y. Choi, and B. H. Kwon, "Cost-effective boost converter with reverse-recovery reduction and power factor correction," *IEEE Transactions on Industrial Electronics*, vol. 55, no. 1, pp. 471-473, Jan. 2008.

[21] M. Muhammad, M. Armstrong, M. A. Elgendy, "Analysis and implementation of high-gain non-isolatedDC–DC boost converter*", IET Power Electronics***,** vol. 10, issue: 11, pp. 1241-1249, sept. 2017.

[22] M. Mohammadi, E. Adib, and H. J. I. P. E. Farzanehfard, "Lossless passive snubber for a double ended flyback converter with the passive clamp circuit," *IET Power Electronics*, vol. 7, no. 2, pp. 245-250, Jan. 2014.

[23] N. Elsayad, H. Moradisizkoohi, and O. Mohammed, "A Single-Switch Transformerless DC-DC Converter with Universal Input Voltage for Fuel Cell Vehicles: Analysis and Design," *IEEE Transactions on Vehicular Technology*, vol. 68, Issue: 5, pp. 4537 - 4549, March. 2019.

[24] A. I. Pressman, *Switching power supply design*, 2nd ed, New York, NY, USA. McGraw-Hill, 1998.

[25] M. R. Yazdani, H. Farzanehfard, and J. Faiz, "EMI analysis and evaluation of an improved ZCT flyback converter," *IEEE Transactions on Power Electronics,* vol. 26, no. 8, pp. 2326-2334, Aug. 2011.

[26] Y. Sahin, NS Ting, I Aksoy, "Soft switching passive snubber cell for family of PWM DC-DC converters," *Electr. Eng*, pp. 1785-1796, 100, (3), Sep 2018.

Tayyebeh Shamsi was born in Najafabad, Iran, in 1986. She received the B.S. degree in electrical engineering (electronics) from the Shahid Beheshti University, Tehran, Iran, in 2009, and the M.S. degree in electrical engineering (electronics) from the Tarbiat Modares University, Tehran, in 2013. She is currently working toward the Ph.D. degree in electrical engineering at the Isfahan (Khorasgan) Branch, IAU. Her research interest includes soft switching techniques in DC-DC converters

Majid Delshad was born in Isfahan, Iran, in 1979. He received the B.S and M.S degrees in electrical engineering in 2001 and 2004 from Kashan University and Isfahan University of Technology, Iran, respectively. He received the Ph.D degree also in electrical engineering in Isfahan University of Technology. He is associate professor in Isfahan (Khorasgan) Branch, IAU. His research interest includes soft switching techniques in DC-DC converters and current-fed converters.

Ehsan Adib was born in Isfahan, Iran, in 1982. He received the B.S., M.S., and Ph.D. degrees in electrical engineering from the Isfahan University of Technology, Isfahan, in 2003, 2006, and 2009, respectively. He is currently a Faculty Member in the Department of Electrical and Computer Engineering, Isfahan University of Technology. He is the author of more than 50 papers published in journals and conference proceedings. His research interests include dc–dc converters and their applications and soft-switching techniques. Dr. Adib was the recipient of the Best Ph.D. Dissertation Award from the IEEE Iran Section in 2010.

Mohammad Rouhollah Yazdani (M'10) was born in Isfahan, Iran, in 1978. He received the B.S. degree from the Isfahan University of Technology, Isfahan, Iran, in 2001; the M.S. degree from the Islamic Azad University, Najafabad Branch, Isfahan, Iran, in 2004, and the Ph.D. degree from the Sciences and Research Branch, Islamic Azad University, Tehran, Iran, in 2011, all in electrical engineering. Since 2011, he has been a Faculty Member at the Department of Electrical and Computer Engineering, Isfahan (Khorasgan) Branch, Islamic Azad University, Isfahan, Iran. His research interests include soft-switching converters, EMI reduction techniques and EMC issues.